H19 recruited N^6-methyladenosine (m^{6}A) reader YTHDF1 to promote SCARB1 translation and facilitate angiogenesis in gastric cancer

Rumeng Bai[1], Miaomiao Sun[1,2], Yuanyuan Chen[3], Shuaishuai Zhuo[1], Guoxin Song[1], Tianjun Wang[1], Zhihong Zhang[1]

[1]Department of Pathology, The First Affiliated Hospital of Nanjing Medical University, Nanjing, Jiangsu 210029, China;
[2]Department of Pathology, Wuxi Maternity and Child Health Hospital Affiliated to Nanjing Medical University, Wuxi, Jiangsu 214002, China;
[3]Department of Biochemistry, Nanjing Medical University, Nanjing, Jiangsu 211112, China.

Abstract

Background: Angiogenesis is described as a complex process in which new microvessels sprout from endothelial cells of existing vasculature. This study aimed to determine whether long non-coding RNA (lncRNA) H19 induced the angiogenesis of gastric cancer (GC) and its possible mechanism.

Methods: Gene expression level was determined by quantitative real-time polymerase chain reaction and western blotting. Cell counting kit-8, transwell, 5-Ethynyl-2′-deoxyuridine (EdU), colony formation assay, and human umbilical vein endothelial cells (HUVECs) angiogenesis assay as well as Matrigel plug assay were conducted to study the proliferation, migration, and angiogenesis of GC *in vitro* and *in vivo*. The binding protein of H19 was found by RNA pull-down and RNA Immunoprecipitation (RIP). High-throughput sequencing was performed and next Gene Ontology (GO) as well as Kyoto Encyclopedia of Genes and Genomes (KEGG) analysis was conducted to analyze the genes that are under H19 regulation. Methylated RIP (me-RIP) assay was used to investigate the sites and abundance among target mRNA. The transcription factor acted as upstream of H19 was determined through chromatin immunoprecipitation (ChIP) and luciferase assay.

Results: In this study, we found that hypoxia-induced factor (HIF)-1α could bind to the promoter region of H19, leading to H19 overexpression. High expression of H19 was correlated with angiogenesis in GC, and H19 knocking down could inhibit cell proliferation, migration and angiogenesis. Mechanistically, the oncogenic role of H19 was achieved by binding with the N^6-methyladenosine (m^{6}A) reader YTH domain-containing family protein 1 (YTHDF1), which could recognize the m^{6}A site on the 3′-untransated regions (3′-UTR) of scavenger receptor class B member 1 (SCARB1) mRNA, resulting in over-translation of SCARB1 and thus promoting the proliferation, migration, and angiogenesis of GC cells.

Conclusion: HIF-1α induced overexpression of H19 via binding with the promoter of H19, and H19 promoted GC cells proliferation, migration and angiogenesis through YTHDF1/SCARB1, which might be a beneficial target for antiangiogenic therapy for GC.

Keywords: Gastric cancer; H19 long non-coding RNA; Angiogenesis; YTHDF1 protein, human; SCARB1 protein, human; 6-methyladenine

Introduction

Gastric cancer (GC) is the third leading cause of cancer-related death and the fifth most frequently diagnosed cancer worldwide, and the incidence rates in Eastern Asia occupy the first place worldwide in both sexes.[1,2] To make matters worse, most cases are already in advanced state when they are diagnosed, which is one of the reasons that the 5-year survival rate is so poor.[3] Lymph node metastasis is also the reason for its difficult treatment and poor prognosis. Therefore, a better grasp of mechanism underlying metastasis in GC cells will help identify new approaches to improve treatment efficacy for GC patients.

Access this article online

Quick Response Code:

Website: www.cmj.org

DOI: 10.1097/CM9.0000000000002722

Angiogenesis is described as a complex process, in which new microvessels sprout from endothelial cells in existing vasculature under the action of some factors in the extracellular matrix that are released from cancer cells.[4,5] Soluble factors such as growth factors, cytokines, and chemokines such as angiopoietin-2 (ANGII), vascular endothelial growth factor (VEGF), vasohibin 2 (VASH2), and hypoxia-induced factor (HIF) can promote endothelial cell migration and angiogenesis in an autocrine and/or paracrine manner.[4,6] The imbalance of these factors contributes to the formation of tumor microvessels.[7] The lack of nutrients in solid

Rumeng Bai, Miaomiao Sun, and Yuanyuan Chen contributed equally to this work.

Correspondence to: Zhihong Zhang, Department of Pathology, The First Affiliated Hospital of Nanjing Medical University, 300, Guangzhou Road, Nanjing, Jiangsu 210029, China
E-Mail: zhangzh@njmu.edu.cn

Chinese Medical Journal 2023;136(14)
Received: 06-07-2022; **Online:** 05-06-2023 **Edited by:** Jinjiao Li and Yuanyuan Ji

tumors is one of the important factors that promotes angiogenesis, and molecules of the HIF family play a crucial role in this process. HIF is a heterodimer of an oxygen-regulated α subunit and a stably expressed β subunit. HIFα protein is stabilized and translocates into the nucleus under hypoxic condition, where it dimerizes with HIFβ, allowing the heterodimer to bind hypoxia response elements (HREs) and then activate the transcription of downstream target genes.[8,9]

Long non-coding RNAs (lncRNAs) are determined as transcripts larger than 200 nucleotides that participate in many biological activities, such as apoptosis, cell differentiation, metastasis, and angiogenesis, thus contributing to cancer progression.[3,10] *H19*, located in 11p15.5 was found decades ago and acts as oncogene in various cancers. Previous studies have verified that H19 promoted glioma cell proliferation, migration, and angiogenesis via the miR-342/Wnt5a/β-catenin axis which provided a new therapeutic target for glioma treatment.[11,12] Although several studies have reported that H19 regulates angiogenesis in cancers, its mechanism needs to be further explored.

In mammalian cells, N^6-methyladenosine (m^6A) is the most prevalent modification of mRNA and is a dynamic RNA modification and this kind of modification can influence various biological functions, including mRNA structure, maturation, and stability.[13,14] Nevertheless, there are few reports on the study of m^6A in GC and its regulatory relationship with angiogenesis-related factors. This study aimed to elucidate the effect of HIF-1α/H19/YTH protein 1 (YTHDF1)/scavenger receptor class B member 1 (SCARB1) axis in the proliferation, migration and angiogenesis process of GC cells.

Methods

Ethical approval

This study was performed strictly in accordance with the recommendations in the Guide for the Care and Use of Laboratory Animals of the National Institutes of Health (1601248-4). The protocol was approved by the Animal Ethical and Welfare Committee of Nanjing Medical University. Written informed consent was obtained from all patients and this study was approved by the Ethics Committee of the First Affiliated Hospital of Nanjing Medical University (2017-SRFA-049). All operations complied with the *Declaration of Helsinki*.

Human tissues and tissue microarrays

Fresh tumor samples as well as adjacent tumor samples were collected from 48 GC patients operated in the First Affiliated Hospital of Nanjing Medical University from December 2018 to July 2019. Clinical and pathological data were integrated including gender, age, tumor size, pathologic tumor node metastasis (pTNM), lymph node metastasis, general classification, and Lauren's classification. All samples were not treated with radiotherapy, chemotherapy or other therapy aimed at tumors. We reviewed the whole hematoxylin–eosin (H&E) stained sections of the 48 patients and selected the representative cores including GC areas and regular tissue areas for tissue microarray analysis. Tissue microarray blocks were divided into GC blocks and normal tissue blocks which were constructed by the diameter of 1.5 mm representative cores taken from formalin-fixed paraffin-embedded (FFPE) tissue using the Manual Tissue Arrayer (Beecher Instruments, Sun Prairie, WI, USA).

Cell lines and cell culture

The human GC cell lines BGC-823, AGS, SGC-7901, MKN-45, and NCI-N87 were cultured in RPMI-1640, GES-1 was cultured in Dulbecco's modified Eagle's medium (DMEM, Gibco, Life Technologies, Carlsbad, CA, USA), and human umbilical vein endothelial cells (HUVECs) were cultured in Endothelial Cell Medium (ECM, ScienCell, Santiago, USA). All media were supplemented with 10% fetal bovine fetal (FBS, AusGeneX, Brisbane, Australia) and 1% penicillin and streptomycin (Invitrogen Co., Ltd., Carlsbad, CA, USA), and incubation condition was 37°C with 5% CO_2.

Transfection

We constructed sh-H19 for *in vivo* experiments using pRNA1.1-Neo-GFP-U6 vector. The sequence and the details of small interfering RNA (siRNA) as well as sh-H19 were listed in Supplementary Table 3, http://links.lww.com/CM9/B581. Lip3000 (Invitrogen Co., Ltd., Carlsbad, CA, USA) and FuGENE® HD Transfection Reagent (Promega Corporation, Wisconsin, USA) were used to transfect si-H19 and overexpression plasmid targeted H19 (pcDNA-H19) and their corresponding control sequences, respectively, after dilution with Opti-MEM™ Reduced Serum Medium (opti-MEM) (Gibco, USA).

Extraction of RNA and quantitative Real-time Polymerase Chain Reaction (qRT-PCR)

Total RNA was extracted from tissues and cells using TRIzol reagent (Invitrogen Co., Ltd., Carlsbad, CA, USA), trichloroethane, and isopropanol. To determine the expression level of mRNA, we used PrimeScript™ RT reagent Kit with genomic DNA (gDNA) Eraser (Perfect Real Time) (Takara, Shiga, Japan) to reverse transcription into cDNA. After this, qRT-PCR was conducted with TB Green Premix Ex Taq™ (Tli RNaseH Plus) (Takara, Japan). The primer sequences were listed in Supplementary Table 1, http://links.lww.com/CM9/B581.

Cell proliferation assay

Cells were seeded into a 96-well plate after transfection for 24 h and added 10 μL/well CCK8 (Bimake, Houston, USA) for every 24 h, and the plate was incubated for 2 h in 37°C. Then the absorbance was measured at 450 nm. Colony formation assay was performed using a 6-well plate that was seeded the same amount of treatment or control cells and incubated for 2 weeks before crystal violet staining. 5-Ethynyl-2′-deoxyuridine (EdU) assay

was also used to examine the ability of cell proliferation according to the manufacturer's instructions (Ribobio, Guangzhou, China).

Transwell migration assay

To verify the ability of cell migration, we conducted a transwell assay using a 24-well plate and transwell chambers (Corning Incorporated, New York, USA). After transfection for 24 h, 300 μL cell suspension (15,000 cells/well) were seeded into the upper chambers while the lower chambers were added 700 μL medium with FBS. After incubation at 37°C for 48 h, the chambers along with the cells were stained by crystal violet before methanol fixation for 30 min. Then we counted the number of cells passing through the basement membrane.

Angiogenesis assay in vitro

After the GC cells were transfected with si-H19/si-SCARB1/si-HIF-1α or pcDNA-H19 for 24 h, a new complete medium was changed and continue culturing for 24 h. The supernatant was collected and centrifuged at 4°C to remove cell debris and other impurities. Human umbilical vein endothelial cells (HUVECs) were planted on the Matrigel Matrix (Corning, Shanghai, China) at a density of 20,000 cells per well in a 96-well gel plate. The same volume of GC cell supernatant was added into the 96-well plate for co-incubation, then we observed and taken pictures at an appropriate time. Tube numbers were analyzed by Image J software (http://rsb.info.nih.gov/ij/).

Nuclear/cytoplasmic separation assay

The nuclear/cytoplasmic separation assay was performed to determine the subcellular localization of H19 and the experiment process was performed according to the manufacturer's instructions (Life Technologies, CA, USA). The internal reference included β-actin which was mainly expressed in cytoplasm and U6 which was mainly expressed in nucleus.

In vivo assay and Matrigel plug assay

Four weeks female BALB/c-nude mice were purchased from Charles River (Beijing, China). shRNA control (empty vector) and sh-H19 were transfected into BGC-823 cells for 24 h. The cells were collected after digested by trypsin. The cells were washed using phosphate buffered saline (PBS) (Gibco, USA) twice and resuspended with PBS before being subcutaneously injected into nude mice. When we conducted the Matrigel plug assay, we mixed the hypertension matrigel matrix (Corning, Shanghai, China) with cell suspension and then subcutaneously injected it into nude mice using the same method as above. The longest and shortest diameters of tumors were measured every 3 days. The tumor volume was calculated according to the formula: tumor volume (mm^3) = (the longest diameter × the shortest diameter^2)/2. The mice were sacrificed after 2 weeks, then H&E and immunohistochemistry (IHC) staining were conducted.

IHC

FFPE tissues of the subcutaneous tumors were cut into 4 μm tissue slices before being deparaffinized and rehydrated for 15 min. Antigen repair was conducted by ethylene diamine tetra acetic acid (EDTA) loading buffer under high pressure. Sections were incubated with primary antibodies at 4°C overnight. Secondary antibody was added and incubated at room temperature for 17 min. Incubated with 3,3-N-diaminobenzidine tetrahydrochloride (DAB) for 3–5 min, sections were counterstained with hematoxylin followed by differentiation, dehydration, transparency, and sealing. The details of the antibodies were listed in Supplementary Table 2, http://links.lww.com/CM9/B581.

High-throughput sequencing

To investigate the downstream target genes regulated by lncRNA H19, we conducted a microarray analysis. H19 siRNA was transfected into BGC-823 cell lines for 24 h and then lysing cells with TRIzol. High-throughput sequencing was performed and next Gene Ontology (GO) as well as Kyoto Encyclopedia of Genes and Genomes (KEGG) analysis was conducted to analyze the genes that are under H19 regulation.

RNA pulldown assay and mass spectrometer analysis

A biotin-coupled H19 probe (sense and antisense) was specially designed using Thermo Scientific Pierce™ RNA 3′ End Desthiobiotinylation Kit (Thermo Fisher Scientific, Waltham, MA, USA). Cell lysate of BGC-823 cells was prepared using Thermo Scientific Pierce IP Lysis Buffer (Thermo Fisher Scientific, Waltham, MA, USA). Incubated cell lysate with 50 pmol biotin-labeled probes and streptavidin magnetic beads for 1 hour. After eluting the protein, mass spectrometry was used to detect the proteins binding with H19.

RNA immunoprecipitation (RIP)

RIP assay was conducted according to Magna RIP™ RNA-Binding Protein Immunoprecipitation Kit (Millipore, USA). In general, cell lysate using RIP Lysis Buffer with protease inhibitor cocktail and RNase inhibitor was essential for the experiment. After rotating protein A/G magnetic beads with IgG or anti-YTHDF1 [Supplementary Table 2, http://links.lww.com/CM9/B581] for 30 min at room temperature, cell lysate was incubated with antibody-beads mixture for at least 6 h. And then RNA was eluted, purified and resuspended with RNase-free water. Next, qRT-PCR was used to quantitatively detect the RNA (H19 and SCARB1) binding to YTHDF1.

Methylated RNA immunoprecipitation (Me-RIP)

Total RNA was extracted using FastPure® Cell/Tissue Total RNA Isolation Mini Kit (Vazyme, Nanjing, China). Next Me-RIP assay was according to the protocol of Magna MeRIP™ m^{6}A Kit (Millipore, Billerica, MA, USA). Breifly, the total RNA extracted from cells were fragmented into 100–200 bp, and the methylated RNA

was extracted through the magnetic bead–m^{6}A antibody–RNA complex. The abundance of m^{6}A was quantitatively detected by qRT-PCR. The primers that were used were listed in Supplementary Table 1, http://links.lww.com/CM9/B581.

Chromatin immunoprecipitation (ChIP)

Chromatin with formaldehyde (1% final concentration) (BOSTER Biological Technology, Wuhan, China) was cross-linked for 10 min at 37°C and cells were collected. According to nuclear lysis buffer in Magna CHIP™ Kit (Millipore, Billerica, MA, USA), cell pellets were resuspended and then nuclear lysate was sonicated to shear DNA to an average length between 200 and 1000 bp. Cell lysate was incubated with protein A/G magnetic beads and primary antibody of HIF-1α for immunoprecipitated. qRT-PCR was performed directly after DNA elution. Primer sequence that was used was listed in Supplementary Table 1, http://links.lww.com/CM9/B581.

Western blotting

The total proteins were isolated with radio-immunoprecipitation assay (RIPA) lysis buffer (Beyotime, Shanghai, China). The proteins were transferred to polyvinylidene fluoride (PVDF) (Millipore, Billerica, MA, USA) membrane after electrophoresis on SDS-PAGE. Incubated with antibodies. The signal was developed using enhanced chemiluminescence (ECL) fluid (Beyotime, China). The antibodies used were listed in Supplementary Table 2, http://links.lww.com/CM9/B581.

Dual-luciferase assay

Wild-type (WT) and mutant-type (MUT) plasmids of HRE1 and /HRE2 plasmids were constructed. HIF-1α siRNA and HRE1/HRE2 double reporter gene carrier (WT) or MUT) was transfected into BGC-823 and AGS cell lines for 24 h and then cells were lysed. The activity of luciferase was tested according to the protocol of Dualucif® Firefly & Renilla Assay Kit (US EVERBRIGHT®INC, Suzhou, China).

Statistical analysis

All statistical analyses were performed by SPSS 17.0 software (IBM, Armonk, NY, USA). Relationships between clinicopathologic parameters were calculated by the chi-squared test. P <0.05 was chosen for statistical significance. Statistical analysis data were expressed as the mean of three experiments ± standard deviation.

Results

H19 was highly expressed and was associated with angiogenesis in GC

Solid tumors such as GC often show obvious angiogenesis. We performed immunohistochemical staining of the vascular marker CD34 in 30 pairs of GC and adjacent normal tissues using microarray. The CD34-positive site was the cytoplasm of vascular endothelial cells and the blood vessels were cord-shaped or had obvious lumens. The microvessel density (MVD) per unit area was used to assess MVD [Figure 1A]. We identified a clear angiogenesis trend in GC compared with the normal gastric epithelium [Figure 1B]. LncRNAs have been reported to participate in regulating the angiogenesis of tumors and H19 can promote the angiogenesis of glioma.[4,15] The role of H19 in GC has been studied, but its mechanisms still need to be further explored.[16] Using the bioinformatics network TANRIC (https://ibl.mdanderson.org/tanric/_design/basic/main.html), we first predicted that the expression level of H19 in GC is significantly increased compared to that in normal tissues [Figure 1C], and the overall survival of patients with high H19 expression was significantly lower than that of those with low H19 expression ($P = 0.019$) (data from: http://gepia.cancer-pku.cn/) [Figure 1D]. Subsequently, the expression of H19 was verified in 48 pairs of fresh GC tissues and adjacent normal tissues [Figure 1E], and the results showed that H19 expression was significantly increased in 37 pairs of GC tissues and was positively correlated with MVD [Figure 1F]. We divided 48 GC patients into the H19 low expression group ($n = 24$) and the H19 high expression group ($n = 24$). The correlation between the expression of H19 and clinicopathological parameters (including gender, age, tumor size, pTNM stage, Lauren's classification, and lymph node metastasis) showed no significant difference, but the expression of H19 showed obvious correlation with general classification [Table 1]. We next verified the expression level of H19 in various human GC cell lines (including BGC-823, AGS, SGC-7901, MKN-45, NCI-N87, and MGC-803) as well as a normal gastric epithelial cell line (GES-1), and the results suggested that H19 was highly expressed in BGC-823 cells and moderately expressed in AGS and SGC-7901 cells [Figure 1G].

H19 promoted the proliferation, migration, and angiogenesis of GC cells in vitro

SiRNA (si-H19) and an overexpression plasmid (pcDNA-H19) were constructed, and the expression level of H19 was significantly reduced after transfection with si-H19 in BGC-823 and AGS cells. The pcDNA-H19 plasmid led to overexpression in SGC-7901 and AGS cells [Figure 2A, B]. Next, we performed functional experiments such as CCK8, colony formation, EdU, transwell and HUVECs angiogenesis assay to verify that H19 knockdown could reduce GC cell proliferation, migration, and angiogenesis *in vitro*, while overexpression of H19 by pcDNA-H19 had the opposite effects [Figure 2C–H and Supplementary Figure 1A–D, http://links.lww.com/CM9/B581]. We then used qRT-PCR to determine the expression of downstream genes related to angiogenesis, including matrix metallopeptidase 9 (MMP9), vascular endothelial growth factor A (VEGFA), and ANGII, after transfection with si-H19, and pcDNA-H19, and found that expression of these genes were changed along with H19 expression [Figure 2I, J]. Our preliminary research proved that H19 was upregulated in GC tissues and cell lines compared with normal controls. H19 expression

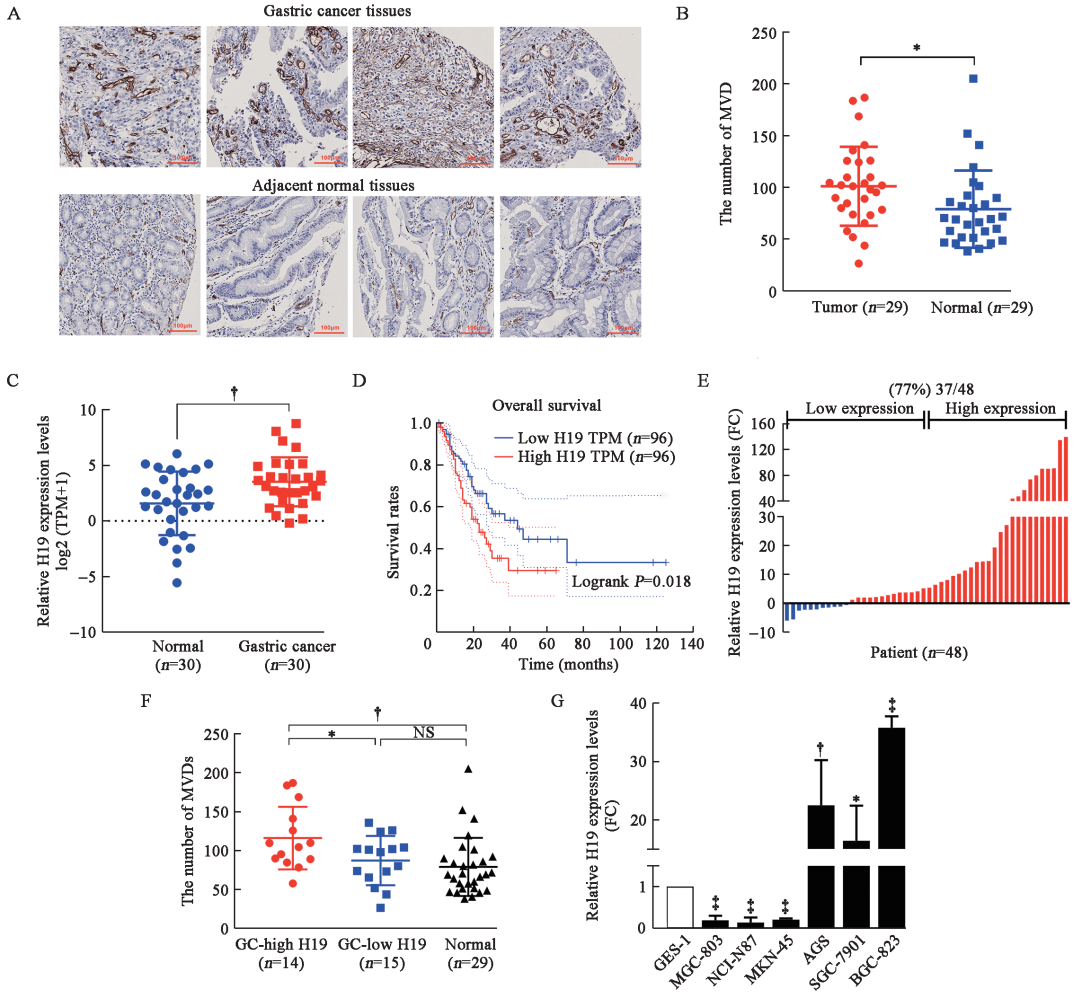

Figure 1: H19 was overexpressed in GC and was correlated with angiogenesis in GC patient. (A) The immunohistochemical staining of CD34 in GC tissues and the adjacent normal tissues. Bar: 100 μm. (B) The MVD in GC was higher than adjacent normal tissues. (C) H19 was elevated in GC in TCGA database (TANRIC). (D) GEPIA database showed that H19 was negatively related to OS in GC patients. (E) H19 was up-regulated in 37 of 48 GC tissues compared to adjacent normal tissues. (F) The MVD of patients with H19 high expression was significantly higher than H19 low expression and normal gastric epithelial tissues. (G) The expression level of H19 in GC cell lines and GES-1. $^{*}P$ <0.05, $^{\dagger}P$ <0.01, $^{\ddagger}P$ <0.001, FC: Fold change; GC: Gastric cancer; MVD: Microvessel density; NS: Not significant; OS: Overall survival; GES-1: Human gastric mucosal epithelial cells; TPM: Transcripts per million.

was positively correlated with MVD in GC and H19 knockdown could inhibit the proliferation, migration, and angiogenesis of GC cells *in vitro*.

H19 promoted the proliferation, migration, and angiogenesis of GC cells in vivo

Given that we have verified that H19 could promote the proliferation, migration, and angiogenesis of GC cells *in vitro*, we wanted to further verify whether H19 could play the same role *in vivo*. We next constructed a plasmid targeting H19 (sh-H19) that could markedly downregulate H19 expression [Figure 3A]. Nude mice were subcutaneously injected with BGC-823 cells transfected with sh-H19 for 24 h. As expected, H19 significantly reduced the proliferation ability of BGC-823 cells *in vivo* [Figure 3B] according to a significant reduction in tumor weight and tumor volume [Figure 3C,D]. Next, qRT-PCR was conducted to confirm that the H19 expression level was also suppressed [Figure 3E]. H&E and IHC staining of Ki-67 indicated significant inhibition of tumor proliferation *in vivo* [Figure 3F]. On the other hand, we employed a mouse Matrigel plug angiogenesis assay and mice were also subcutaneously injected with Matrigel plugs containing BGC-823 cells transfected with either sh-H19 or empty vector. The Matrigel plug angiogenesis assay showed that BGC-823 cells transfected with sh-H19 presented a significant decrease in blood vessel formation ability *in vivo* [Figure 3G]. There were fewer microvessels containing red blood cells (RBCs) which are marked by green arrows, in the Matrigel plugs of the H19 knockdown group than in those of the empty vector group [Figure 3H]. IHC staining of the angiogenesis markers CD34 and VEGF also showed a significant reduction after sh-H19 transfection [Figure 3H]. Taken together, these results indicated that H19 could promote the proliferation, migration, and angiogenesis of GC *in vivo*.

Table 1: Correlation between clinicopathological characteristics and H19 expression level.

Clinicopathological parameters	H19 expression level		χ^2	*P* value
	High expression (*n* = 24)	Low expression (*n* = 24)		
Gender			1.613	0.204
Male	15	19		
Female	9	5		
Age			0.083	0.773
≤65 years	12	11		
>65 years	12	13		
Tumor size			0.087	0.768
≤5 cm	14	15		
>5 cm	10	9		
pTNM stage			0.091	0.763
I–II	8	9		
III–IV	16	15		
General classification			4.547	0.033
Ulcer type	16	22		
Non-ulcer type	8	2		
Lauren's classification			3.286	0.193
Intestinal type	6	12		
Diffuse type	8	6		
Mixed type	10	6		
Vascular tumor thrombus			3.000	0.083
No	9	15		
Yes	15	9		
Lymph node metastasis			0	1.000
No	5	5		
Yes	19	19		

SCARB1 is up-regulated in GC tissues as a downstream of H19 and promoted proliferation, migration, and angiogenesis of GC

To further study the downstream target genes regulated by H19, we performed high-throughput sequencing after knocking down H19 in BGC-823 cells and found that 89 genes were differentially expressed in all three si-H19 repeat groups and the genes were mostly downregulated [Figure 4A, B]. We assessed the expression levels of 12 significantly downregulated factors of interest in BGC-823 and AGS cells after knocking down H19, and the most downregulated gene in both cell lines was *SCARB1* [Supplementary Figure 2A,B, http://links.lww.com/CM9/B581]. We further verified that the mRNA level of SCARB1 decreased significantly after H19 knockdown in BGC-823 and AGS cells and increased after H19 was overexpressed in SGC-7901 and AGS cells. The scavenger receptor class B type I (SR-BI) encoded by *SCARB1* showed the same results [Figure 4C, D]. Data in the TCGA database showed a significant upregulation of SCARB1 in GC and a positive correlation between SCARB1 and H19 [Supplementary Figure 2C, D, http://links.lww.com/CM9/B581]. These results were consistent with those of our experimental assay in 48 GC tissues [Figure 4E, F and Supplementary Figure 2E, http://links.lww.com/CM9/B581].

We constructed a small interfering RNA targeting SCARB1 (si-SCARB1), which could significantly reduce its mRNA and protein expression in GC cells after exploration of the expression level of SCARB1 in several GC cell lines as well as GES-1 [Supplementary Figure 2F, G, http://links.lww.com/CM9/B581]. We further performed *in vitro* experiments to assess the function of SCARB1. CCK8, colony formation assay, EdU, transwell, and HUVECs angiogenesis assay indicated that the proliferation, migration, and angiogenesis of GC cells after SCARB1 knockdown were significantly reduced [Figure 4G and Supplementary Figure 3A–E, http://links.lww.com/CM9/B581]. Next, rescue experiments showed that SCARB1 knockdown could partially eliminate the cancer-promoting effect of H19 on proliferation, migration, and angiogenesis [Figure 4H–J and Supplementary Figure 3F, http://links.lww.com/CM9/B581]. These results indicated that SCARB1 acts as a downstream of H19, and was upregulated in GC tissues and promotes proliferation, migration, and angiogenesis of GC.

H19 recognized the m^{6}A site on SCARB1 mRNA through YTHDF1 to promote SCARB1 translation

Our previous study found that H19 could affect the mRNA and protein expression of SCARB1. To further study the mechanism by which H19 regulates SCARB1, we conducted a nuclear/cytoplasmic separation assay and found that H19 was mainly located in the cytoplasm [Figure 5A], which was consistent with the literature.[17] We used an RNA pull-down and mass spectrometry assay to explore the proteins that interacted with H19 directly in the BGC-823 cells, and YTHDF1 showed obvious direct binding [Figure 5B and Supplementary Figure 4A, http://links.lww.com/CM9/B581]. RIP

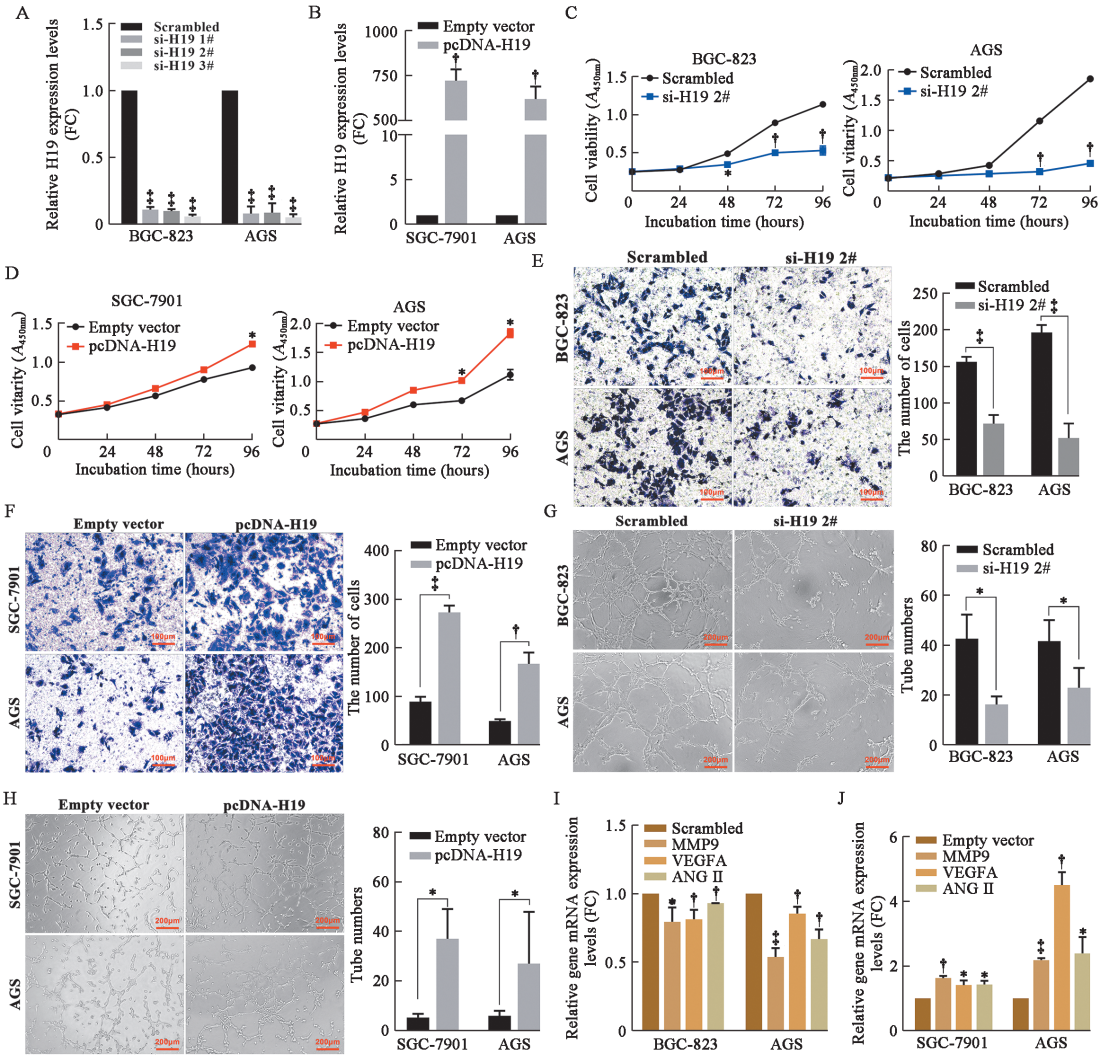

Figure 2: H19 could promote the proliferation, migration, and angiogenesis of GC cells *in vitro*. (A) Both si-H19 1#, 2#, and 3# could reduce the expression level of H19 in BGC-823 and AGS cell lines. (B) The expression of H19 was up-regulated after transfecting with pcDNA-H19 plasmid in SGC-7901 and AGS. (C,D) CCK8 proliferation assays after transfection of si-H19 (C) and pcDNA-H19 plasmid (D). (E, F) The transwell assay after transfection of si-H19 (E) and pcDNA-H19 plasmid (F) by crystal violet staining. Bar: 100 μm. (G, H) The angiogenesis assay after transfection of si-H19 (G) and pcDNA-H19 plasmid (H). Bar: 100 μm. (I,J) The expression level of the relative genes of angiogenesis including VEGFA, MMP9, ANGII after transfection of si-H19 (I) and pcDNA-H19 plasmid (J). $^{*}P$ <0.05, $^{\dagger}P$ <0.01, $^{\ddagger}P$ <0.001. ANGII: Angiopoietin-2; FC: Fold change; CCK8: Cell counting kit-8; GC: Gastric cancer; VEGFA: Vascular endothelial growth factor A.

experiments further proved the combination of YTHDF1 with H19 and SCARB1 mRNA in BGC-823 cells [Figure 5C, D], but H19 did not influence either the mRNA or protein levels of YTHDF1 [Figure 5E, F]. Existing literature has shown that YTHDF1 could recognize methylation sites on mRNA, thereby promoting the translation of downstream target genes.[18] We suspect that H19 can promote the translation of downstream target genes by binding to YTHDF1.

YTHDF1 knockdown decreased the protein level of both YTHDF1 and SR-BI, but did not affect SCARB1 mRNA levels [Supplementary Figure 4B and Figure 5G, H, http://links.lww.com/CM9/B581]. YTHDF1 knockdown partially reversed the increase in expression of SR-BI caused by pcDNA-H19 [Figure 5I and Supplementary Figure 4C, D, http://links.lww.com/CM9/B581]. Since studies have shown that YTHDF1 can promote the translation of downstream target genes mainly by recognizing the m^{6}A site in the 3′-untransated regions (3′-UTR) of mRNA, and then recruit translation initiation factors to form a complex thus promoting gene translation.[19] Me-RIP assay was conducted to verify the location and abundance of m^{6}A on SCARB1 mRNA as described in the methods [Figure 5J]. These results indicated that YTHDF1 protein could recognize the m^{6}A site in the 3′-UTR of SCARB1 mRNA and promote the translation of SCARB1 into SR-BI, thereby exerting GC angiogenesis in which H19 played a penetrating role [Figure 5K]. In summary, we proved that H19 promoted the proliferation, migration, and angiogenesis of GC cells through YTHDF1/SCARB1.

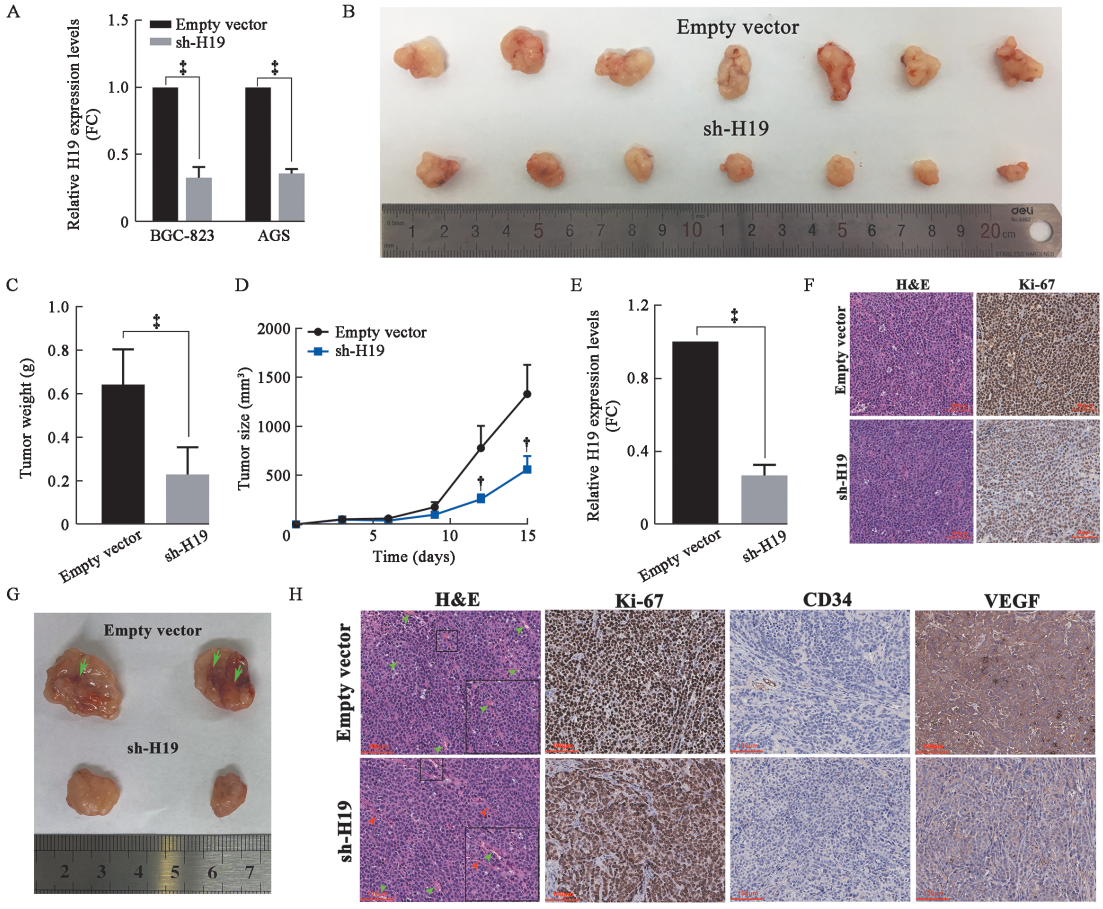

Figure 3: H19 could promote the proliferation, migration, and angiogenesis of GC cells *in vivo*. (A) sh-H19 plasmid could reduce the expression level of H19 in BGC-823 and AGS cells. (B) Xenograft tumors derived from BGC-823 cells with H19 knockdown. (C) Tumor weight of xenograft tumors after 2 weeks. (D) Tumor size measured every 3 days. (E) The H19 expression level in the xenograft tumors transfected with sh-H19 *vs.* empty vector. (F) H&E and IHC staining of Ki-67 in xenograft tumors. Bar: 100 μm. (G) Matrigel plug assay indicated that the angiogenesis was downregulated after H19 knockdown *in vivo*. The arrows of green indicated the blood vessels on the surface of the tumors. (H) Tumors of Matrigel plugs assay were stained with H&E, Ki-67, CD34, and VEGF antibodies. Short arrows of green indicated the matured microvessels which containing RBC and the red arrows showed the microvessels unmatured. Bar: 100 μm. $^{\dagger}P$ <0.01, $^{\ddagger}P$ <0.001. FC: Fold change; GC: Gastric cancer; H&E: hematoxylin–eosin; IHC: Immunohistochemistry; RBC: Red blood cells; VEGF: Vascular endothelial growth factor.

HIF-1α upregulated the expression of H19 by binding to the promoter region of H19 and promoting angiogenesis of GC

Thus far, we have studied the mechanism by which downstream H19 regulates the angiogenesis of GC, but the upstream H19 needs to be further explored. Hypoxia can promote angiogenesis in the process of tumorigenesis and development, so we considered whether the ability of H19 to promote angiogenesis in GC was initiated by HIF. We detected the expression levels of HIF-1α, HIF-2α, and HIF-3α in the TCGA and GC tissues and cell lines. The results indicated that HIF-1α showed a significantly high expression in GC tissues and cell lines [Figure 6A–D] and only knocking down HIF-1α could significantly reduce the expression of H19 in BGC-823 and AGS cells [Figure 6E and Supplementary Figure 4E–G, http://links.lww.com/CM9/B581]. It has been reported that HIF-1α can transcriptionally activate the expression of H19 and elevate the downstream miR-612/Bcl-2 pathway to promote cholangiocarcinoma.[20] We next confirmed that the expression of HIF-1α was positively correlated with the expression of H19 and MVD in GC [Figure 6F,G]. JASPAR (http://jaspar.genereg.net/) was used to predict that there were two HIF-1α binding sites (HRE1 and HRE2) in the promoter region of H19. Dual-luciferase assays and ChIP experiments verified that HIF-1α could bind to the promoter region of H19 directly in BGC-823 and AGS cells and transcriptionally upregulate H19 in GC [Figure 6H–J].

Functional experiments *in vitro* showed that knocking down HIF-1α could significantly inhibit the proliferation, migration, and angiogenesis of BGC-823 and AGS cells [Supplementary Figure 5A–D, http://links.lww.com/CM9/B581]. Rescue experiments showed that overexpression of H19 reversed the downregulated proliferation, migration, and angiogenesis caused by knocking down HIF-1α [Supplementary Figure 5E–H, http://links.lww.com/CM9/B581]. HIF-1α could act as the upstream of H19 by binding to HREs in the promoter, thus promoting the expression of H19 and played the role of a pro-oncogene in GC cells.

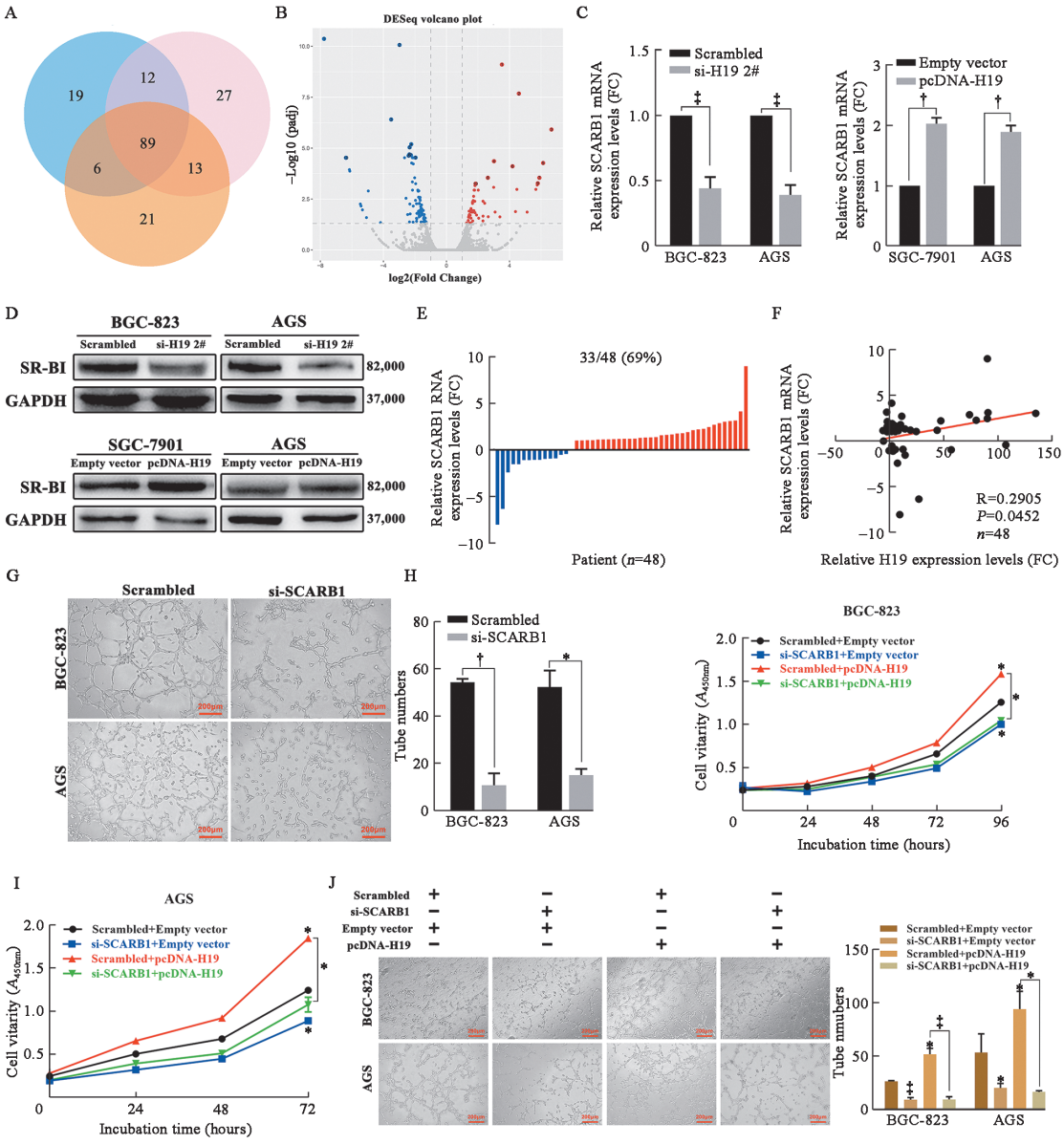

Figure 4: SCARB1 was up-regulated in GC tissues and could promote the proliferation, migration, and angiogenesis of GC. (A) High-throughput sequencing revealed that 89 genes were differentially expressed in all three repetition groups with H19 knockdown in BGC-823 cell lines. (B) Volcano plot of high-throughput sequencing. (C,D) The mRNA and protein level of SCARB1 in GC cell lines was down-regulated after transfected with si-H19 while up-regulated transfected with pcDNA-H19 plasmid. (E) SCARB1 mRNA was highly expressed in 33 of 48 pairs of GC tissues compared to adjacent normal tissues. (F) There was a positive correlation between the expression of H19 and SCARB1 in 48 GC tissues. (G) The angiogenesis assay after transfection of si-SCARB1 in BGC-823 and AGS cell lines. Bar: 200 μm. (H–J) Rescue assay of CCK8 and angiogenesis by co-transfection of si-SCARB1 and pcDNA-H19 in BGC-823 and AGS cells. Bar: 200 μm. $^{*}P$ <0.05, $^{\dagger}P$ <0.01, $^{\ddagger}P$ <0.001. FC: Fold change; CCK8: Cell counting kit-8; GC: Gastric cancer; SR-BI: Scavenger receptor class B type I.

Discussion

Invasive tumor growth and metastasis rely on angiogenesis, which allows vessels to effectively deliver nutrients and remove metabolic wastes.[21,22] Angiogenic switch is turned on surprisingly early in the development of invasive cancer when proangiogenic factors such as VEGF become dominant over antiangiogenic factors.[22] LncRNAs play pivotal roles of angiogenesis especially in tumors, and previous studies revealed that H19, which is upregulated by oxidative stress could regulate cell migration and invasion via competing endogenous RNA mechanisms involving sponging of targeting genes such as Bcl2 and VASH2, thus suppressing tumor angiogenesis.[4,20] Zhao *et al*[21] clarified that plasmacytoma variant translocation 1 (PVT1) could bind to nuclear phosphorylated signal transducer and activator of transcription 3 (p-STAT3) protein, thus protecting it from poly-ubiquitin-proteasomal degradation to enhance the activation of STAT3 signaling pathway, thereby increasing VEGF expression to induce angiogenesis. Bao *et al*[23] proved that LINC00657 acts as a miR-590-3p sponge to attenuate the suppressive effect of miR-590-3p on HIF-1α and then promotes angiogenesis through VEGF, matrix metallopeptidase 2 (MMP2), and MMP9. Our previous study

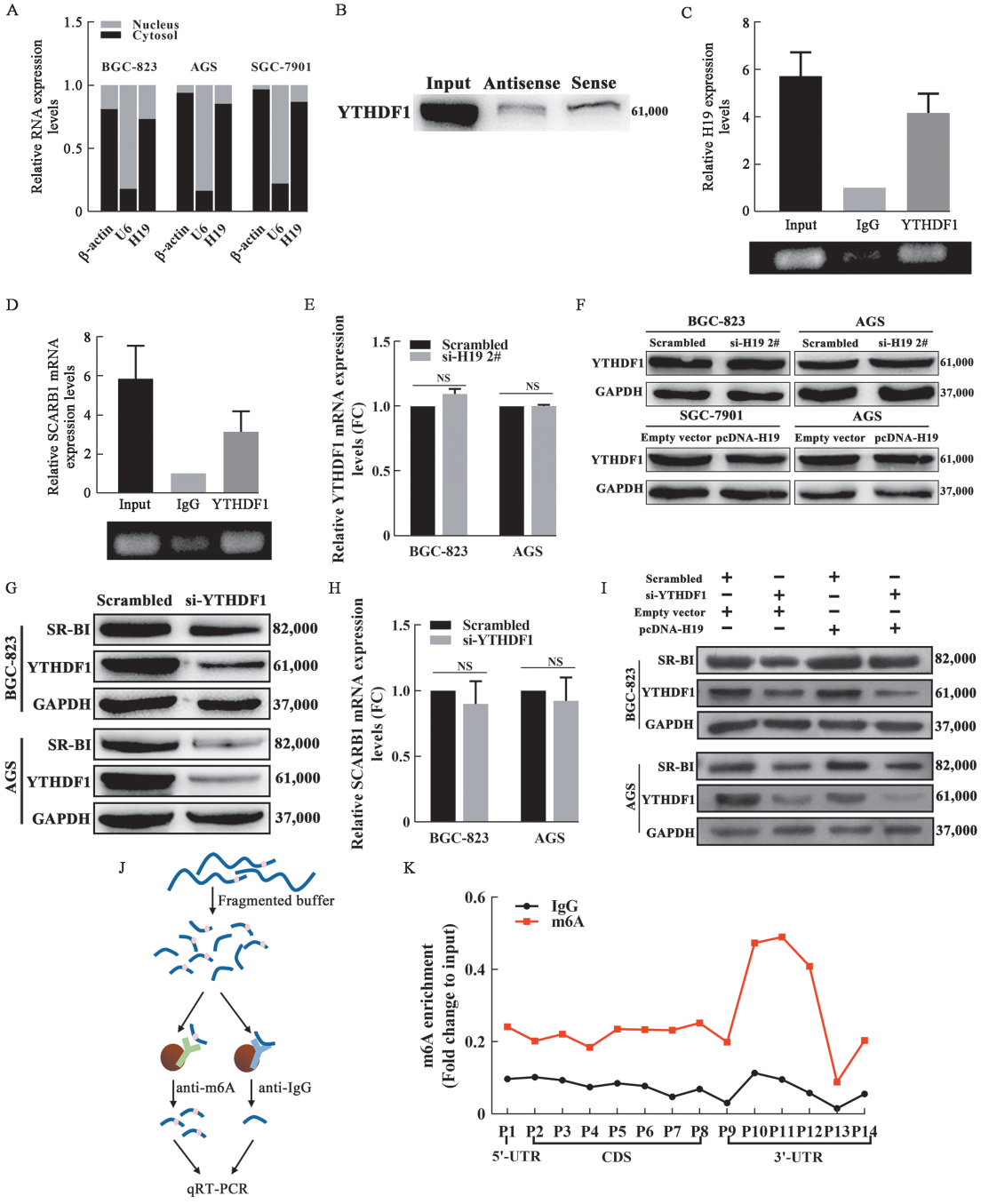

Figure 5: H19 recognized the m^{6}A site on SCARB1 mRNA through YTHDF1 thus promoting SCARB1 translation. (A) Nuclear/cytoplasmic separation assay was conducted to determine that H19 was mainly localized in cell plasma of BGC-823, AGS, and SGC-7901 cell lines. (B) RNA pulldown-western blotting was used to verify that H19 could bind to YTHDF1 directly. (C,D) RIP assays for YTHDF1 were performed and qRT-PCR was used to examine H19 (C) and SCARB1 mRNA (D). (E,F) Knockdown of H19 in BGC-823 and AGS cells did not affect the expression of YTHDF1 both in mRNA and protein level. (G,H) YTHDF1 knockdown could reduce the expression of SR-BI in protein without mRNA change. (I) The western blotting was conducted to detect the protein level of SR-BI after co-transfection with si-YTHDF1 and pcDNA-H19 in BGC-823 and AGS cell lines. (J,K) Me-RIP experiments and qRT-PCR methods were conducted to determine that the location and abundance of m^{6}A mainly in 3′-UTR on SCARB1 mRNA. FC: Fold change; me-RIP: Methylated RNA immunoprecipitation; NS: Not significant; qRT-PCR: Quantitative real-time polymerase chain reaction; RIP: RNA Immunoprecipitation; SR-BI: Scavenger receptor class B type I; 3′-UTR: 3′-untransated regions; 5′-UTR: 5′-untransated regions; CDS: Coding sequence; SCARB1: Scavenger receptor class B member 1; YTHDF1: YTH domain-containing family protein 1.

revealed that the expression of HIF-1α is positively correlated with the level of angiogenesis and the expression of H19 in GC. Knocking down HIF-1α could definitely inhibit the expression of H19 by binding to HREs in the H19 promoter region.

Although H19 is known for its role in GC, further studies are required to more rigorously determine the role of H19 in GC angiogenesis.[24] We found that H19 showed high expression in GC and the results were the same as the bioinformatics analysis which was related to

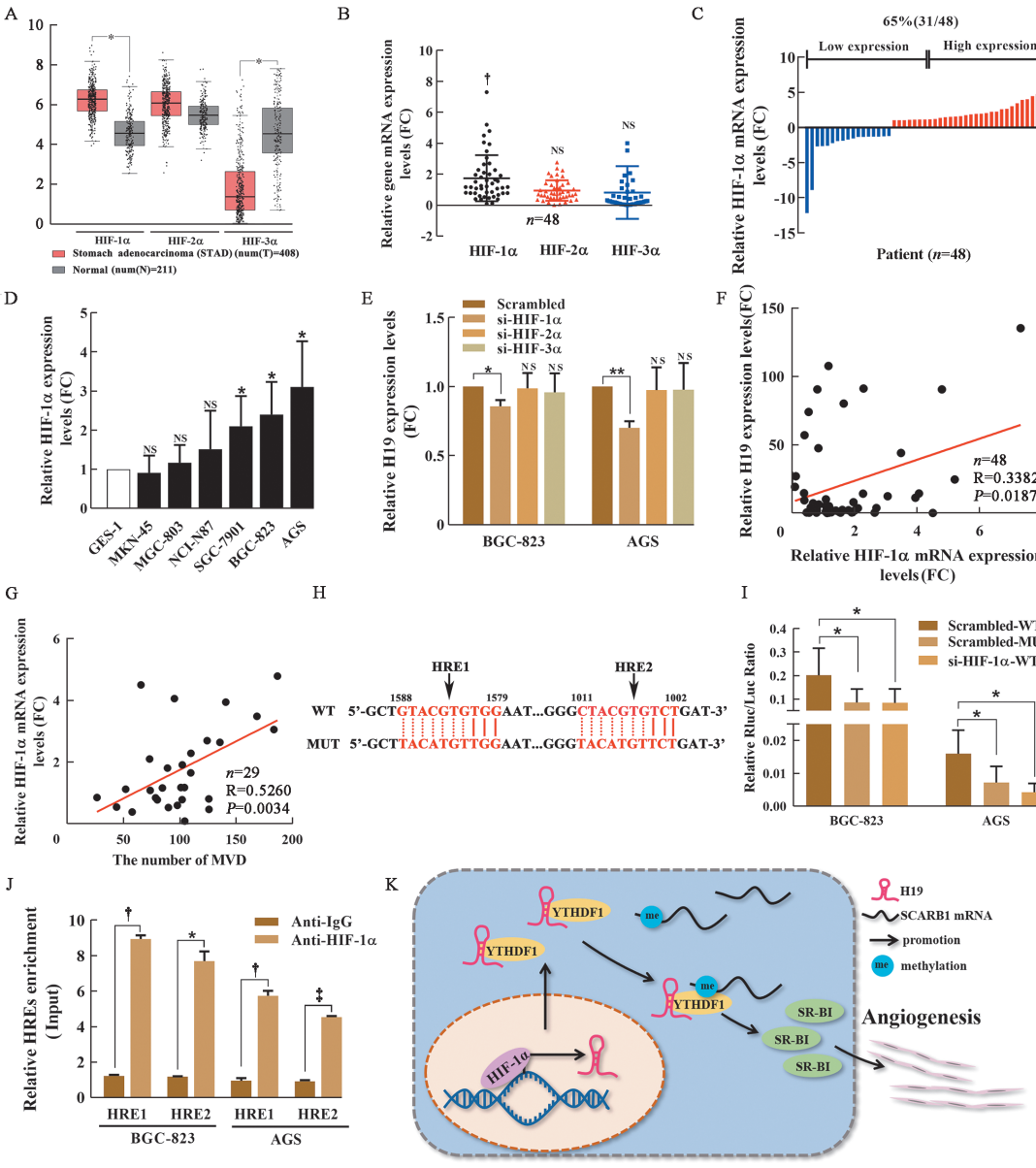

Figure 6: HIF-1α promoted the expression of H19 by binding to the promoter region of H19 and promoted angiogenesis of GC. (A) The expression levels of HIF-1α, HIF-2α, and HIF-3α in TCGA. The red columns represented tissues of stomach adenocarcinoma (STAD) and the gray columns represented normal tissue. (B) The expression levels of HIF-1α, HIF-2α, and HIF-3α in 48 GC tissues. (C) HIF-1α was up-regulated in 31 of 48 GC tissues compared to adjacent normal tissues. (D) The expression levels of HIF-1α in GC cell lines and GES-1. (E) HIF-1α knockdown could reduce the expression level of H19 in GC cells compared with si-HIF-2α and si-HIF-3α. (F) The expression level of HIF-1α was positively correlated with H19 in 48 GC tissues. (G) The expression level of HIF-1a was positively correlated with MVD in 29 GC tissues. (H) The predicted binding sites between HIF-1α and H19 promoter. (I) Luciferase activity in BGC-823 and AGS cells after co-transfecting with si-HIF-1α and luciferase reporters including WT and MUT. Data were presented as the relative ratio of firefly luciferase activity to renal luciferase activity. (J) ChIP assay was conducted in BGC-823 and AGS cells to prove that HIF-1α can bind with the HREs which were existed in the promoter of H19. (K) Summary of HIF-1α target H19 promotes angiogenesis through YTHDF1/SCARB1 in GC. Statistical analysis data were expressed as the mean of three experiments ± standard deviation, $^{*}P$ <0.05, $^{\dagger}P$ <0.01, $^{\ddagger}P$ <0.001, FC: Fold change; ChIP: Chromatin Immunoprecipitation; GC: Gastric cancer; HIF-1α: Hypoxia-inducible factor 1α; HIF-2α: Hypoxia-inducible factor 2α; HIF-3α: Hypoxia-inducible factor 3α; GES-1: Human gastric mucosal epithelial cells; HREs: Hypoxia response elements; MUT: Mutant type; MVD: Microvessel density; NS: Not significant; WT: Wild type; SCARB1: Scavenger receptor class B member 1; YTHDF1: YTH domain-containing family protein 1.

the general classification and MVD of patients. Knocking down H19 could significantly reduce the proliferation, migration, and angiogenesis of GC both *in vitro* and *in vivo*. *SCARB1* was the downstream target gene of H19 which was highly expressed in GC. The *SCARB1* gene encodes SR-BI, which is an 82,000 glycoprotein with two transmembrane domains associated with two intracellular N-termini and C-termini and an extracellular glycosylated central domain which mediates the selective high-density lipoprotein-cholesterol (HDL-C) uptake of cells.[25,26] The mechanisms by which H19 regulates SCARB1 to promote GC angiogenesis need further exploration.

As mentioned above, current researche on H19 has focused on its ability to act as a molecular sponge to adsorb

miRNAs and free downstream target genes to perform corresponding biological functions in tumor cells.[27,28] H19 binding protein is lack of research. YTHDF1 was identified as an H19 binding protein in our previous research, which could identify m^{6}A in the 3′-UTR of mRNA and promote the translation of target genes. m^{6}A is the most prevalent internal modification for eukaryotic mRNA and influences nearly every stage of RNA metabolism, including splicing, decay, export, and translation.[29] YTHDF1 is a key regulator of m^{6}A methylation and can accelerate the translational output of Frizzled 5 (FZD5) and FZD7 mRNA in a m^{6}A-dependent manner and function as an oncogene through Wnt signaling.[18,30] Studies have clarified the role of YTHDF1 in delivering cellular mRNAs to the translation machinery to facilitate translation initiation directly. YTHDF1 can act with translation initiation complexes including eukaryotic initiation factor (eIF) 3, eIF4G, and eIF4E which can bind both cap and poly(A) of mRNA to form a "closed loop," and then translation initiation complex initiaties translation of target genes.[31] In the pathological process, m^{6}A methylation is dynamically required for maintaining the functions and characteristics of tumor cells during tumorigenesis and development.[32] Previous studies have shown that m^{6}A is catalyzed by a multicomponent protein complex consisting of the "writers" including methyltransferase-like 3/14 (METTL3/14) and Wilms tumor 1-associated protein (WTAP), among which METTL3 methyltransferase is the key catalytic subunit.[19,33] The study of Zhao *et al*[34] determined that METTL3 targets the 3′-UTR (near to stop codon) of c-Myc to install the m^{6}A modification, thereby enhancing the stability of c-Myc and enhancing YTHDF1-mediated translation. In our study, m^{6}A was found to be significantly enriched in the 3′-UTR of SCARB1 mRNA. The results of me-RIP assay verified our conjecture that H19 regulated the protein of SR-BI through YTHDF1-mediated translation in GC.

Nevertheless, the mechanism of YTHDF1 and m^{6}A inducing deregulation of SCARB1, and other possible relationship between H19 and SCARB1 remain to be further investigated. Our findings have identified novel potential therapeutic targets for GC. But this research still has some limitations, such as the specific binding sites of YTHDF1 with H19 and SCARB1. As a high-density lipoprotein (HDL) receptor, whether SCARB1 regulated metabolism of HDL cholesterol and the details of SCARB1 downstream mechanism in regulating the development of GC still needs further research. Future studies should examine the specific binding sites on H19/SCARB1 and the mechanism of SCARB1 in regulating the development of GC.

In conclusion, our study proved that HIF-1α could bind to HREs in the promoter region of H19, thus promoting the transcription of H19, and enhancing angiogenesis mediated by H19. High H19 expression in GC could promote proliferation, migration, and angiogenesis both *in vitro* and *in vivo*. Mechanically, H19 could directly bind with YTHDF1 which could recognize m^{6}A in the 3′-UTR of SCARB1 mRNA and then facilitate translation of SCARB1 into SR-BI which also played an oncogenic role in GC. This research showed the mechanisms of HIF-1α/H19/YTHDF1/SCARB1 in the regulation of GC angiogenesis, and provided a detailed description of the m^{6}A-related mechanism of GC metastasis.

Acknowledgments

All authors thank Nanjing Xinjia Medical Technology Co. Ltd (China) for providing technical platform support. All authors thank Dr. Wei De (Department of Biochemistry and Molecular Biology, Nanjing medical university, Nanjing, Jiangsu Province, China) for guiding the research work.

Conflicts of interest

The authors declare no competing interest.

References

1. Shuai Y, Ma Z, Liu W, Yu T, Yan C, Jiang H, *et al*. TEAD4 modulated LncRNA MNX1-AS1 contributes to gastric cancer progression partly through suppressing BTG2 and activating BCL2. Mol Cancer 2020;19:6. doi: 10.1186/s12943-019-1104-1.
2. Xia C, Dong X, Li H, Cao M, Sun D, He S, *et al*. Cancer statistics in China and United States, 2022: Profiles, trends, and determinants. Chin Med J 2022;135:584–590. doi: 10.1097/cm9.0000000000002108.
3. Li D, Wang J, Zhang M, Hu X, She J, Qiu X, *et al*. LncRNA MAGI2-AS3 is regulated by BRD4 and promotes gastric cancer progression via maintaining ZEB1 overexpression by sponging miR-141/200a. Mol Ther Nucleic Acids 2020;19:109–123. doi: 10.1016/j.omtn.2019.11.003.
4. Jia P, Cai H, Liu X, Chen J, Ma J, Wang P, *et al*. Long non-coding RNA H19 regulates glioma angiogenesis and the biological behavior of glioma-associated endothelial cells by inhibiting microRNA-29a. Cancer Lett 2016;381:359–369. doi: 10.1016/j.canlet.2016.08.009.
5. Lin J, Cao S, Wang Y, Hu Y, Liu H, Li J, *et al*. Long non-coding RNA UBE2CP3 enhances HCC cell secretion of VEGFA and promotes angiogenesis by activating ERK1/2/HIF-1alpha/VEGFA signalling in hepatocellular carcinoma. J Exp Clin Cancer Res 2018;37:113. doi: 10.1186/s13046-018-0727-1.
6. Deng F, Zhou R, Lin C, Yang S, Wang H, Li W, *et al*. Tumor-secreted dickkopf2 accelerates aerobic glycolysis and promotes angiogenesis in colorectal cancer. Theranostics 2019;9:1001–1014. doi: 10.7150/thno.30056.
7. Sang LJ, Ju HQ, Liu GP, Tian T, Ma GL, Lu YX, *et al*. LncRNA Camk-A regulates Ca^{2+}-signaling-mediated tumor microenvironment remodeling. Mol Cell 2018;72:71–83.e7. doi: 10.1016/j.molcel.2018.08.014.
8. Niu Y, Bao L, Chen Y, Wang C, Luo M, Zhang B, *et al*. HIF2-induced long noncoding RNA RAB11B-AS1 promotes hypoxia-mediated angiogenesis and breast cancer metastasis. Cancer Res 2020;80:964–975. doi: 10.1158/0008-5472.CAN-19-1532.
9. Wang X, Wang Y, Li L, Xue X, Xie H, Shi H, *et al*. A lncRNA coordinates with Ezh2 to inhibit HIF-1alpha transcription and suppress cancer cell adaption to hypoxia. Oncogene 2020;39:1860–1874. doi: 10.1038/s41388-019-1123-9.
10. Xu H, Zhao G, Zhang Y, Jiang H, Wang W, Zhao D, *et al*. Long non-coding RNA PAXIP1-AS1 facilitates cell invasion and angiogenesis of glioma by recruiting transcription factor ETS1 to upregulate KIF14 expression. J Exp Clin Cancer Res 2019;38:486. doi: 10.1186/s13046-019-1474-7.
11. Jiang X, Yan Y, Hu M, Chen X, Wang Y, Dai Y, *et al*. Increased level of H19 long noncoding RNA promotes invasion, angiogenesis, and stemness of glioblastoma cells. J Neurosurg 2016;2016:129–136. doi: 10.3171/2014.12.JNS1426.test.
12. Zhou Q, Liu ZZ, Wu H, Kuang WL. LncRNA H19 promotes cell proliferation, migration, and angiogenesis of glioma by regulating Wnt5a/beta-catenin pathway via targeting miR-342. Cell Mol Neurobiol 2020;42:1065–1077. doi: 10.1007/s10571-020-00995-z.

13. Zhang C, Zhang M, Ge S, Huang W, Lin X, Gao J, *et al*. Reduced m6A modification predicts malignant phenotypes and augmented Wnt/PI3K-Akt signaling in gastric cancer. Cancer Med 2019;8:4766–4781. doi: 10.1002/cam4.2360.
14. Jia R, Chai P, Wang S, Sun B, Xu Y, Yang Y, *et al*. m^{6}A modification suppresses ocular melanoma through modulating HINT2 mRNA translation. Mol Cancer 2019;18:161. doi: 10.1186/s12943-019-1088-x.
15. Liu ZZ, Tian YF, Wu H, Ouyang SY, Kuang WL. LncRNA H19 promotes glioma angiogenesis through miR-138/HIF-1α/VEGF axis. Neoplasma 2020;67:111–118. doi: 10.4149/neo_2019_190121N61.
16. Sun L, Li J, Yan W, Yao Z, Wang R, Zhou X, *et al*. H19 promotes aerobic glycolysis, proliferation, and immune escape of gastric cancer cells through the microRNA-519d-3p/lactate dehydrogenase A axis. Cancer Sci 2021;112:2245–2259. doi: 10.1111/cas.14896.
17. Jiang X, Yan Y, Hu M, Chen X, Wang Y, Dai Y, *et al*. Increased level of H19 long noncoding RNA promotes invasion, angiogenesis, and stemness of glioblastoma cells. J Neurosurg 2016;124:129–136. doi: 10.3171/2014.12.JNS1426.
18. Liu X, Qin J, Gao T, Li C, He B, Pan B, *et al*. YTHDF1 facilitates the progression of hepatocellular carcinoma by promoting FZD5 mRNA translation in an m6A-dependent manner. Mol Ther Nucleic Acids 2020;22:750–765. doi: 10.1016/j.omtn.2020.09.036.
19. Liu S, Li G, Li Q, Zhang Q, Zhuo L, Chen X, *et al*. The roles and mechanisms of YTH domain-containing proteins in cancer development and progression. Am J Cancer Res 2020;10:1068–1084.
20. Yu A, Zhao L, Kang Q, Li J, Chen K, Fu H. Transcription factor HIF-1α promotes proliferation, migration, and invasion of cholangiocarcinoma via long noncoding RNA H19/microRNA-612/Bcl-2 axis. Transl Res 2020;224:26–39. doi: 10.1016/j.trsl.2020.05.010.
21. Zhao J, Du P, Cui P, Qin Y, Hu C, Wu J, *et al*. LncRNA PVT1 promotes angiogenesis via activating the STAT3/VEGFA axis in gastric cancer. Oncogene 2018;37:4094–4109. doi: 10.1038/s41388-018-0250-z.
22. Dong F, Ruan S, Wang J, Xia Y, Le K, Xiao X, *et al*. M2 macrophage-induced lncRNA PCAT6 facilitates tumorigenesis and angiogenesis of triple-negative breast cancer through modulation of VEGFR2. Cell Death Dis 2020;11:728. doi: 10.1038/s41419-020-02926-8.
23. Bao MH, Li GY, Huang XS, Tang L, Dong LP, Li JM. Long noncoding RNA LINC00657 acting as a miR-590-3p sponge to facilitate low concentration oxidized low-density lipoprotein-induced angiogenesis. Mol Pharmacol 2018;93:368–375. doi: 10.1124/mol.117.110650.
24. Ghafouri-Fard S, Esmaeili M, Taheri M. H19 lncRNA: Roles in tumorigenesis. Biomed Pharmacother 2020;123:109774. doi: 10.1016/j.biopha.2019.109774.
25. Gutierrez-Pajares JL, Ben Hassen C, Chevalier S, Frank PG. SR-BI: Linking cholesterol and lipoprotein metabolism with breast and prostate cancer. Front Pharmacol 2016;7:338. doi: 10.3389/fphar.2016.00338.
26. Xu GH, Lou N, Shi HC, Xu YC, Ruan HL, Xiao W, *et al*. Up-regulation of SR-BI promotes progression and serves as a prognostic biomarker in clear cell renal cell carcinoma. BMC Cancer 2018;18:88. doi: 10.1186/s12885-017-3761-z.
27. Wang WT, Ye H, Wei PP, Han BW, He B, Chen ZH, *et al*. LncRNAs H19 and HULC, activated by oxidative stress, promote cell migration and invasion in cholangiocarcinoma through a ceRNA manner. J Hematol Oncol 2016;9:117. doi: 10.1186/s13045-016-0348-0.
28. Zhang L, Cheng H, Yue Y, Li S, Zhang D, He R. H19 knockdown suppresses proliferation and induces apoptosis by regulating miR-148b/WNT/beta-catenin in ox-LDL-stimulated vascular smooth muscle cells. J Biomed Sci 2018;25:11. doi: 10.1186/s12929-018-0418-4.
29. Chen XY, Zhang J, Zhu JS. The role of m^{6}A RNA methylation in human cancer. Mol Cancer 2019;18:103. doi: 10.1186/s12943-019-1033-z.
30. Pi J, Wang W, Ji M, Wang X, Wei X, Jin J, *et al*. YTHDF1 promotes gastric carcinogenesis by controlling translation of *FZD7*. Cancer Res 2021;81:2651–2665. doi: 10.1158/0008-5472.CAN-20-0066.
31. Wang X, Zhao BS, Roundtree IA, Lu Z, Han D, Ma H, *et al*. N(6)-methyladenosine modulates messenger RNA translation efficiency. Cell 2015;161:1388–1399. doi: 10.1016/j.cell.2015.05.014.
32. Sun T, Wu Z, Wang X, Wang Y, Hu X, Qin W, *et al*. LNC942 promoting METTL14-mediated m^{6}A methylation in breast cancer cell proliferation and progression. Oncogene 2020;39:5358–5372. doi: 10.1038/s41388-020-1338-9.
33. Liu T, Wei Q, Jin J, Luo Q, Liu Y, Yang Y, *et al*. The m6A reader YTHDF1 promotes ovarian cancer progression via augmenting EIF3C translation. Nucleic Acids Res 2020;48:3816–3831. doi: 10.1093/nar/gkaa048.
34. Zhao W, Cui Y, Liu L, Ma X, Qi X, Wang Y, *et al*. METTL3 facilitates oral squamous cell carcinoma tumorigenesis by enhancing c-Myc stability via YTHDF1-mediated m^{6}A modification. Mol Ther Nucleic Acids 2020;20:1–12. doi: 10.1016/j.omtn.2020.01.033.

How to cite this article: Bai RM, Sun MM, Chen YY, Zhuo SS, Song GX, Wang TJ, Zhang ZH. H19 recruited N^6-methyladenosine (m^{6}A) reader YTHDF1 to promote SCARB1 translation and facilitate angiogenesis in gastric cancer. Chin Med J 2023;136:1719–1731. doi: 10.1097/CM9.0000000000002722